

# Reactions of $ZnR_2$ Compounds with Dibenzoyl: Characterisation of the Alkyl-Transfer Products and a Striking Product-Inhibition Effect

Izabela Dranka,<sup>[a]</sup> Marcin Kubisiak,<sup>[a]</sup> Iwona Justyniak,<sup>[b]</sup> Michał Lesiuk,<sup>[a]</sup>  
Dominik Kubicki,<sup>[a]</sup> and Janusz Lewiński\*<sup>[a, b]</sup>

Dedicated to Professor Janusz Jurczak on the occasion of his 70th birthday

**Abstract:** The first systematic theoretical and experimental studies of reaction systems involving  $ZnR_2$  ( $R=Me$ ,  $Et$  or  $tBu$ ) with dibenzoyl (dbz) as a non-innocent ligand revealed that the character of the metal-bonded  $R$  group as well as the ratio of the reagents and the reaction temperature significantly modulate the reaction outcome. DFT calculations showed four stable minima for initial complexes formed between  $ZnR_2$  and dbz and the most stable structure proved to be the 2:1 adduct; among the 1:1 adducts three structural isomers were found of which the most stable complex had the monodentate coordination mode and the chelate complex with the *s-cis* conformation of

the dbz unit appeared to be the least stable form. Interestingly, the reaction involving  $ZnMe_2$  did not lead to any alkylation product, whereas the employment of  $Zn*t*Bu_2$  resulted in full conversion of dbz to the *O*-alkylated product [ $tBuZn[PhC(O)C(O*t*Bu)Ph]$ ] already at  $-20^\circ C$ . A more complicated system was revealed for the reaction of dbz with  $ZnEt_2$ . Treatment of a solution of dbz in toluene with one equivalent of  $ZnEt_2$  at room temperature afforded a mixture of the *O*- and *C*-alkylated

products [ $EtZn[PhC(O)C(OEt)Ph]$ ] and [ $EtZn[OC(Ph)C(O)(Et)Ph]$ ], respectively. The formation of the *C*-alkylated product was suppressed by decreasing the initial reaction temperature to  $-20^\circ C$ . Moreover, in the case of the dbz/ $ZnEt_2$  system monitoring of the dbz conversion over the entire reaction course revealed a product inhibition effect, which highlights possible participation of multiple equilibria of different zinc alkoxide/ $ZnEt_2$  aggregates. Diffusion NMR studies indicated that dbz forms an adduct with the *O*-alkylated product, which is a competent species for executing the inhibition of the alkylation event.

**Keywords:** alkoxides • alkylation • ketones • structure–activity relationships • zinc

## Introduction

The influence of a zinc alkoxide product on the rate and/or course of various reactions involving dialkylzinc reagents and carbonyl compounds is an important issue of synthetic chemistry.<sup>[1]</sup> The most spectacular example concerns the Soai autocatalytic asymmetric addition of diisopropylzinc to pyrimidinyl aldehydes,<sup>[1b,d]</sup> where both the role of the zinc alkoxide product and the structural model of the catalytic centre have been the subject of intense investigations in the last decade.<sup>[2]</sup> In the latter system, the presence of dimers and higher aggregates of the alkoxides and their adducts with diisopropylzinc have been assumed as the key molecular

structures essential in the autocatalytic cycle and the amplification process. It is also peculiar that in another fundamental reaction, the asymmetric alkylation of benzaldehyde by  $ZnEt_2$ ,<sup>[3]</sup> the noticed influence of the conversion on the enantioselectivity of the alkoxide product was attributed to product inhibition, but without a clear structural model.<sup>[1c]</sup> In this regard, our group implied the possible participation of multiple equilibria, including a dimeric, tetranuclear aggregate formed between the alkoxide product and  $ZnR_2$  moieties in the donor-functionalised, alcohol-promoted addition of dialkylzinc to aldehydes, which was supported by structurally well-characterised model complexes.<sup>[4]</sup> Undoubtedly, further systematic elucidation of the mechanisms by which carbonyls react with organozinc species is a challenging task and may help to broaden our understanding of these complex reaction systems.

Surprisingly,  $\alpha$ -diketones have not yet been explored in reactions with  $ZnR_2$  or main group-metal alkyls in contrast to the related rich chemistry of their non-innocent *N,N*-type analogues, that is,  $\alpha$ -diimines.<sup>[5]</sup> Formally,  $\alpha$ -diketones can act as bidentate ligands or undergo oxidative addition reactions accepting one or two electrons. Nevertheless, only two metal complexes with a neutral  $\alpha$ -diketone ligand were structurally characterised hitherto<sup>[6]</sup> and the first complex

[a] Dr. I. Dranka, M. Kubisiak, M. Lesiuk, D. Kubicki,  
Prof. Dr. J. Lewiński  
Faculty of Chemistry Warsaw University of Technology  
Noakowskiego 3, 00-664 Warsaw (Poland)  
Fax: (+48)22-234-7279  
E-mail: lewin@ch.pw.edu.pl

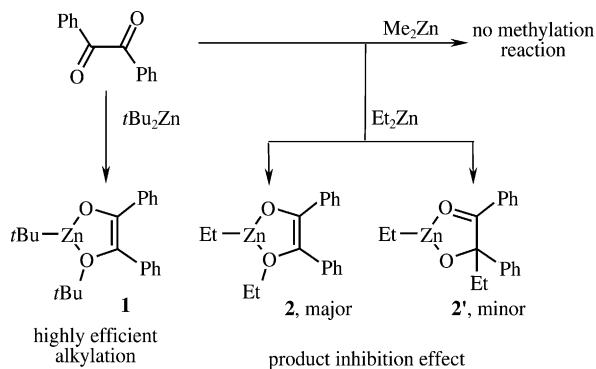
[b] Dr. I. Justyniak, Prof. Dr. J. Lewiński  
Institute of Physical Chemistry Polish Academy of Sciences  
Kasprzaka 44/52, 01-224 Warsaw (Poland)

Supporting information for this article is available on the WWW  
under <http://dx.doi.org/10.1002/chem.201101997>.

with a singly reduced form of an  $\alpha$ -diketone was isolated only recently.<sup>[7]</sup> In the course of our systematic investigation on the structure and reactivity of organozinc complexes, we report herein on the first systematic experimental and theoretical studies of reaction systems involving  $\text{ZnR}_2$  ( $\text{R} = \text{Me}$ ,  $\text{Et}$  or  $t\text{Bu}$ ) with dibenzoyl (dbz). We provide computational evidences for intriguing thermodynamic preference for initial adducts formed between  $\text{ZnR}_2$  and dibenzoyl, as well as the first structurally characterised examples of products of the alkyl transfer reaction from zinc to an  $\alpha$ -diketone. Moreover, we demonstrate a striking zinc alkoxide product inhibition effect with its mechanistic picture. The study also provides an efficient access to alkylzinc enolates,<sup>[8]</sup> which potentially may be further exploited as valuable reagents in organic synthesis<sup>[9]</sup> or initiators in polymerisation processes.<sup>[10]</sup>

## Results and Discussion

Treatment of a solution of dibenzoyl in toluene with one equivalent of  $\text{ZnMe}_2$  resulted in a colour change from light yellow to orange; this observation was the only indication of a complex formation between those reagents and IR spectroscopy appeared to be not a sensitive probe for detecting an equilibrium between the chelated and free dibenzoyl (see the Supporting Information). The reaction did not lead to any methylation products, even after extended periods of time at room temperature. In contrast, employment of  $\text{Zn}t\text{Bu}_2$  resulted in a full conversion of dbz upon mixing of the substrates in toluene already at  $-20^\circ\text{C}$  (Scheme 1). This



Scheme 1. Schematic representation of the reaction products formed in the dbz/ $\text{ZnR}_2$  system at  $20^\circ\text{C}$ .

fast reaction led to the *O*-alkylated product [ $t\text{BuZn}\{\text{PhC}(\text{O})\text{C}(\text{O}t\text{Bu})\text{Ph}\}$ ] (**1**), which was isolated with high yield after a standard work up. The NMR data are fully consistent with the anticipated formula of **1** (see the Supporting Information), which was confirmed by X-ray crystallography (see below).

Unexpectedly, a more complicated system was revealed when we set to investigate the reaction of dbz with  $\text{ZnEt}_2$ . Treatment of a solution of dbz in toluene with one equivalent of  $\text{ZnEt}_2$  at room temperature afforded a mixture of

the *O*- and *C*-alkylated products, [ $\text{EtZn}\{\text{PhC}(\text{O})\text{C}(\text{OEt})\text{Ph}\}$ ] (**2**) and [ $\text{EtZn}\{\text{OC}(\text{Ph})\text{C}(\text{O})\text{Et}\text{Ph}\}$ ] (**2'**), in a 1.5:1 ratio (Scheme 1); as the  $^1\text{H}$  NMR spectrum of the reaction mixture after the reaction is complicated and not informative, the alkylation products were identified spectroscopically after hydrolysis of the crude product (see the Supporting Information for more details). However, the formation of the *C*-alkylated product was suppressed by decreasing the initial reaction temperature to  $-20^\circ\text{C}$  followed by slow warming up to ambient temperature, which resulted in a highly selective formation of the *O*-alkylated product **2** (**2/2'** ratio  $>19:1$ ). The observed divergent pathways of the alkylation reaction affected by the character of the R group are similar to those found in  $\alpha$ -diimine/ $\text{R}_2\text{Zn}$  systems, where the *tert*-butyl reagent tends to alkylate the nitrogen, whereas the ethyl reagent leads to a mixture of *N*- and *C*-alkylated products.<sup>[5a]</sup>

Strikingly, the corresponding experiment in an NMR tube showed that only approximately half of the amount of  $\text{ZnEt}_2$  is consumed initially in the first few minutes (Figure 1a) and in the next 2–3 days the signals assigned to

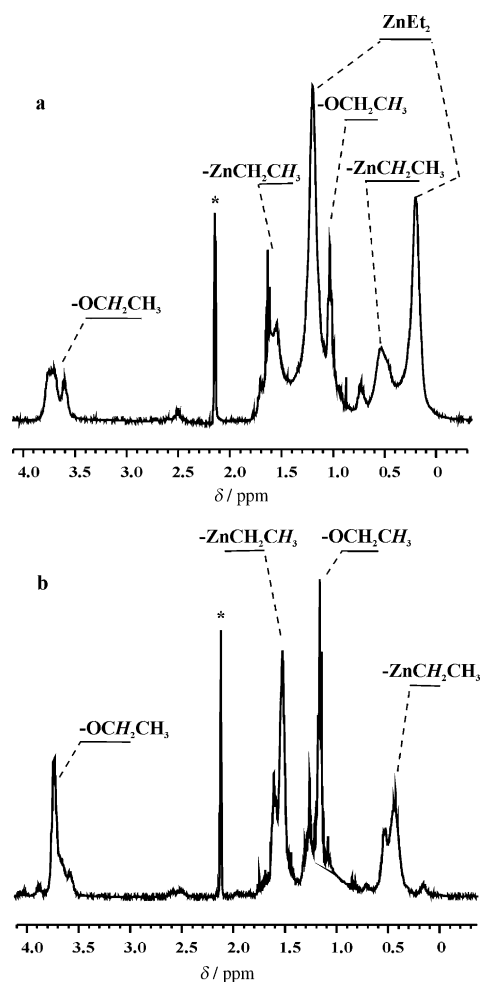


Figure 1.  $^1\text{H}$  NMR spectra for the alkylation of dbz with  $\text{ZnEt}_2$ : a) after 30 min from mixing of the substrates at  $-20^\circ\text{C}$  and warming up to  $20^\circ\text{C}$ ; b) the crude product **2** (\* indicates the residual signal of  $[\text{D}_8]$ toluene residual signal).

ZnEt<sub>2</sub> gradually decrease with concomitant increase of those associated with **2**. The <sup>1</sup>H NMR spectrum of **1** in [D<sub>8</sub>]toluene showed broad signals for the ethoxide group at  $\delta = 1.15$  and 3.78 ppm, associated with the ethoxy-enolate ligand, and the corresponding broad signals of the ZnEt moiety at  $\delta = 0.46$  and 1.51 ppm (Figure 1 b). The observed broadness of all the ethyl group signals apparently reflects fluxional behaviour of the resulting alkylzinc-alkoxide aggregates in solution. Reaction progress for alkylation of dibenzoyl with ZnEt<sub>2</sub> is best expressed by in-situ-monitored conversion of dibenzoyl as a function of time (Figure 2).

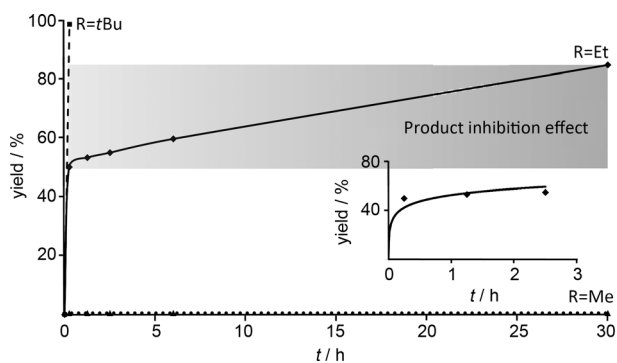


Figure 2. Conversion versus time diagram for the alkylation of dbz with an equimolar amount of ZnR<sub>2</sub> in [D<sub>8</sub>]toluene.

The observed complicated character of the conversion plot of dibenzoyl with an initial steep slope followed by a sharp change to a slower rate could be reasonably explained by the assumption that product **2** forms an adduct with ZnEt<sub>2</sub>, which effectively leads to the inhibition of the alkylation reaction. Previously we have implied the possible participation of multiple equilibria of different Zn aggregates in RZn(O,N)/ZnR<sub>2</sub> systems and suggested the involvement of adducts between alkylzinc alkoxides and ZnR<sub>2</sub> moieties, which was supported by structurally well-characterised model complexes.<sup>[4]</sup> In light of the assumed ZnEt<sub>2</sub> deficiency in the reaction mixture, we subsequently treated dibenzoyl with an excess of ZnEt<sub>2</sub>. Surprisingly, when two or more equivalents of ZnEt<sub>2</sub> were used, the alkylation reaction was further inhibited and repeatedly only a very low conversion (<5% found by NMR spectroscopy) of dibenzoyl to **2** was found.<sup>[11]</sup> This observation clearly indicated that it is not the ZnEt<sub>2</sub> deficiency that blocks the alkylation of dbz but rather its excess. The results forced us to embark on the examination of less obvious parameters.

In order to explore the nature of the species formed in solution between ZnR<sub>2</sub> and dibenzoyl in more detail, we have used density functional theory. Calculations of the structures and their relative energies for the 2:1 and 1:1 adducts were carried out by using the Gaussian 09 program package with the M06-2X functional and the aug-cc-pVTZ basis set level of theory.<sup>[23]</sup> The energy profile for the ZnEt<sub>2</sub>/dbz system is shown in Figure 3 a and the optimised geometries of the key species are given in Figure 3 b. Similar data were obtained

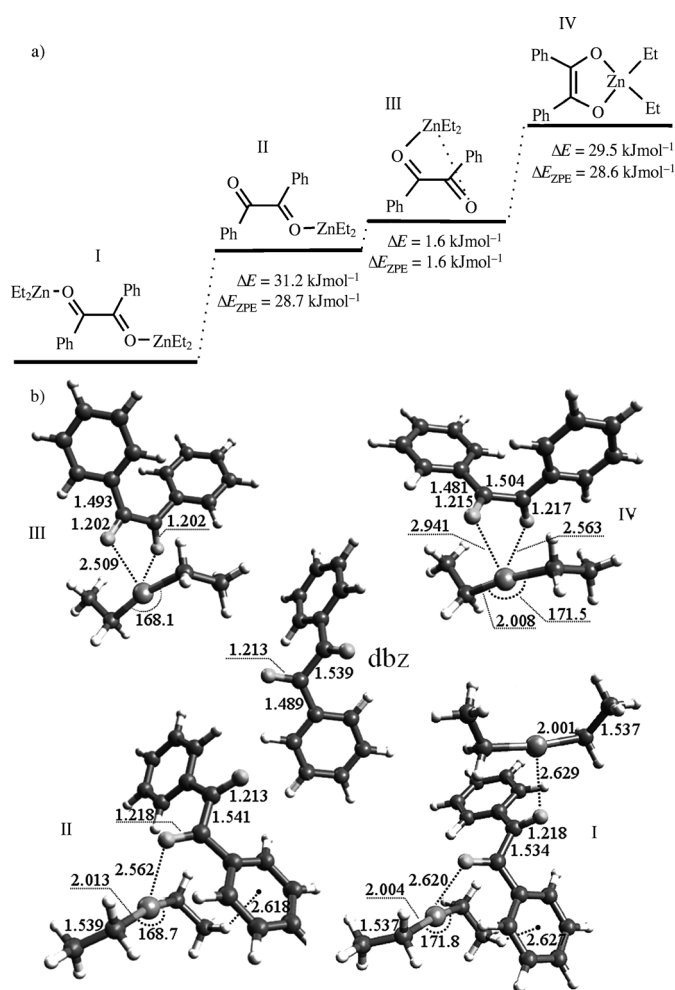


Figure 3. a) Optimised structures of the ZnEt<sub>2</sub> complexes with dbz (ZPE = zero-point energy). b) DFT-calculated relationships between the complexes of ZnEt<sub>2</sub> with dbz.

for the ZnMe<sub>2</sub>/dbz system (for the corresponding data see Figures S3 and S4 in the Supporting Information), therefore below we discuss in detail the diethylzinc adducts. The calculations show four stable minima for adducts formed between ZnEt<sub>2</sub> and dbz, and the most stable structure proves to be the 2:1 adduct I (Figure 3 a). Remarkably, among the 1:1 adducts three structural isomers were found, of which the most stable complex II has a monodentate coordination mode and is 28.7 kJmol<sup>-1</sup> higher in energy than the 2:1 adduct. Another stable minimum for the 1:1 system appeared to be the semi-chelated complex III stabilised by a number of cooperative weak interactions, which was found to be only 1.6 kJmol<sup>-1</sup> higher than the monodentate adduct II. Surprisingly, the chelate complex IV with the *s-cis* conformation of the dbz unit appeared to be the least stable and was calculated as 28.6 kJmol<sup>-1</sup> higher in energy than the monodentate adduct II. Puzzling feature of this calculation is the observed anticlinical conformation of the dbz unit in adducts I–III, which is essentially the same as that found for the free dbz in its ground state<sup>[12]</sup> (Figure 3 b). This intriguing conformation preference was inspected by computing

the barriers for rotation about the central C–C bond, which showed that the anticlinal conformation is more stable (by 39 kJ mol<sup>-1</sup>) than the planar *s-cis* conformation. Thus, this thermodynamic preference of the anticlinal conformation is a key for understanding the energetic relationships among the ZnEt<sub>2</sub> and dibenzoyl adducts and causes the planar *s-cis* chelate adduct IV to be the least stable structure.

Furthermore, all complexes feature relatively long Zn–O distances with the lower limit of 2.50 Å and an essentially linear structure of the ZnEt<sub>2</sub> molecules (with the C–Zn–C angle ranging from 168.1° in the chelate complex to 171.8° in the 2:1 adduct). Some adducts are additionally stabilised by hydrogen-bonding interactions between the π-electron density of the phenyl residues and the hydrogen atoms of the ZnEt moieties (see adduct I and II, Figure 3b). In our opinion, taking all these features into account, it is justified to call adducts formed between ZnR<sub>2</sub> and dbz noncovalent complexes. Finally, it should be stressed that thermodynamically the process of their formation is exothermic by 35.4 kJ mol<sup>-1</sup> for the monodentate complex I, or by 5.3 kJ mol<sup>-1</sup> for the chelate complex IV in the gas phase, and that it is not significantly affected by the nature of R (the corresponding value for analogous adducts with ZnMe<sub>2</sub> are 24.2 and 5.6 kJ mol<sup>-1</sup>, respectively). The energy difference among the structural isomers is below 60 kJ mol<sup>-1</sup>, which indicates that a multitude of species could be simultaneously present in equilibrium. The results demonstrate that the formation of the 2:1 adduct is favoured, which corroborates with the experimental details, that is, an excess of ZnEt<sub>2</sub> should shift the equilibrium towards this dinuclear, monodentate complex, which may nicely explain the observed inhibition of the alkylation reaction with increasing amount of ZnEt<sub>2</sub>. Thus, in these circumstances our preliminary assumption that the formation of an adduct involving product **2** and ZnEt<sub>2</sub> leads to inhibition of the alkylation reaction rather does not match. It is likely that in the monodentate, three-coordinate adduct {PhC(O)C(O)Ph}(ZnEt<sub>2</sub>) the α-diketone unit acts as an innocent ligand and the formation of the chelate complex {κ<sup>2</sup>(O,O)-PhC(O)C(O)Ph}-ZnEt<sub>2</sub> is crucial for further transformations to proceed (see below).

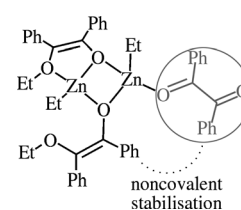
To shed more light on the putative role of the zinc alkoxide product **2** in the observed course of the equimolar reaction, diffusion-ordered NMR spectroscopy (DOSY) investigations on the dibenzoyl/ZnEt<sub>2</sub> system were performed. <sup>1</sup>H DOSY measurements provide a reliable evidence of the approximate size of the species existing in solution. Very recently, it was demonstrated that the molecular weight of the species in question can be straightforwardly obtained by combining the Stokes–Einstein equation [Eq. (1)]:

$$D = (kT)/(6\pi\eta r_H) \quad (1)$$

and the relationship between the molecular weight *M* and the molar radius [Eq. (2)]:

$$M = (4\pi r_M^3 \rho N_A)/3 \quad (2)$$

where *r<sub>H</sub>* and *r<sub>M</sub>* are the hydrodynamic and the molar radius, respectively, *η* is the viscosity and *ρ* is the density of the liquid.<sup>[13]</sup> <sup>1</sup>H DOSY spectra (measured at 293 K) of the solution exhibiting approximately 50% conversion of dbz to **2**, show that all distinct signals assigned to the alkoxide complex have comparable diffusion coefficients *D* = 5.42 × 10<sup>-10</sup> m<sup>2</sup>s<sup>-1</sup>, which gave an estimate of the hydrodynamic radius of 4 Å and further the calculated molecular weight of an aggregate likely formed by **2** of 866 g mol<sup>-1</sup>. The latter value is significantly higher than the formula weight calculated for a dimeric structure of **2** (667.46 g mol<sup>-1</sup>). However, with the formula weights of dbz and ZnEt<sub>2</sub> being 210.23 and 123.50 g mol<sup>-1</sup>, respectively, one can clearly see that the presumptive dimeric structure **2**<sub>2</sub> (2 × (210.23 + 123.50) = 667.46 g mol<sup>-1</sup>) with one dbz molecule involved, gives the total of 667.46 + 210.23 = 877.69 g mol<sup>-1</sup> for the **2**<sub>2</sub>(dbz) adduct, which fairly resembles the experimental data; the putative structure of this adduct is shown on Scheme 2. Thus, the results indicate that dibenzoyl forms an adduct with the alkoxide product **2**, thereby strongly suggesting that the **2**<sub>2</sub>(dbz) adduct is a competent species for executing the inhibition of the alkylation event; the revealed nature of the product inhibition effect for the addition of ZnEt<sub>2</sub> to dbz is opposite in its character to the observed effect for the addition of phenylacetylene to carbonyls promoted by Me<sub>2</sub>Zn where the carbonyl substrate itself was implicated as a ligand facilitating the zinc-mediated addition of alkynes to the substrate.<sup>[14]</sup>



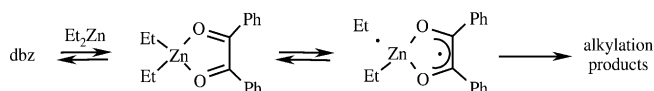
Scheme 2. Proposed structure for the **2**<sub>2</sub>(dbz) adduct as structural model for the dormant species present in the dbz/ZnEt<sub>2</sub> system.

The presumed structure of the **2**<sub>2</sub>(dbz) adduct resembles to some degree the ones observed for **2** and 1,2-bis(4-pyridyl)ethane (see below). This adduct features a non-centrosymmetric dimer with the Zn<sub>2</sub>(μ-O)<sub>2</sub> bridges formed by the enolate oxygen atoms, one chelating and one dangling enolate ligand, and the coordination environment of one zinc centre is completed by a chelating dibenzoyl ligand. It is likely that the adduct formed between the alkoxide product **2** and dbz is additionally stabilised by intramolecular noncovalent interactions involving the phenyl rings and various oxygen centres (see below). It is also worthy to note that the formation of this type of adduct simultaneously supports the formation of the 2:1 adduct between ZnEt<sub>2</sub> and dbz in the parent reaction mixture, according to the Equation (3), which cooperatively should suppress the alkylation reaction.



The observed number of salient features of the dbz/ZnR<sub>2</sub> system allows for mechanistic rationalisation of this intriguing

ing reaction system. As it was mentioned above, the formation of the chelate complex  $\{\kappa^2(\text{O},\text{O})\text{dbz}\}\text{ZnR}_2$  is the first crucial step for the alkylation process. Only for this type of highly organised, four-coordinate chelate complexes the non-innocent character of the dibenzoyl ligand is preserved as a result of the accessibility and symmetry properties of the  $\pi^*$  molecular orbitals, which allows single-electron transfer (SET) from the Zn–C bond (Scheme 3). The subsequent alkyl radical transfer to carbonyl oxygen atom (or carbon atom) of the ligand leads to the alkylated product.



Scheme 3. Alkyl radical transfer following the SET in the ZnR<sub>2</sub>/ $\alpha$ -diketone chelate complex, which leads to the formation of the alkylation products.

All processes in these first stages are fast for ZnEt<sub>2</sub> and Zn*n*Bu<sub>2</sub>, and resemble those proposed for the  $\alpha$ -diimine/ZnR<sub>2</sub> system.<sup>[5]</sup> The observed lack of dbz alkylation by ZnMe<sub>2</sub> is likely due to the character of the Zn–Me bond, which is less prone to the single-electron transfer (e.g., a similar effect was observed for the reactions with  $\alpha$ -diimines<sup>[15]</sup>) as the formation of the initial chelate complex is not significantly affected by the nature of R (see above). Furthermore, in the second slow distinct stage, the alkylated product traps dbz to form an aggregate, which leads to the observed inhibition of the alkylation reaction. In our opinion, the observed differences in the dbz conversion mediated by ZnEt<sub>2</sub> and Zn*n*Bu<sub>2</sub> are an additional instance that highlights the role of an intermediate adduct between the resulting *O*-alkylated species and the carbonyl substrate. The putative intermediate aggregate between **1**<sub>2</sub> and dbz is likely to be unstable due to steric encumbrances and does not affect the alkylation reaction. These observations are in line with another type of product inhibition effect disclosed recently by our group in the course of the oxygenation of alkylzinc chelate complexes, where the resulting alkylperoxide species and the parent alkylzinc complex formed an adduct.<sup>[16]</sup> Only destabilisation of this type of adducts, for example, by introduction of steric encumbrances led to the complete oxygenation of the Zn–C bonds.<sup>[17]</sup>

The identity of the alkylated products has been confirmed by X-ray crystallography (Figure 4). Although the *tert*-butylated product **1** easily crystallises from a solution of THF/hexane, attempts to grow crystals of the *O*-ethylated product **2** were unsuccessful due to its excellent solubility in non-coordinating solvents. Nevertheless, our group has recently demonstrated that a combination of *N,N*-linkers with well-soluble organometallic entities provides a convenient method for entrapment of elusive species in form of various extended assemblies.<sup>[18]</sup> Given this experience, treatment of a solution of **2** with 0.5 equivalent (per zinc) of 1,2-bis(4-pyr-

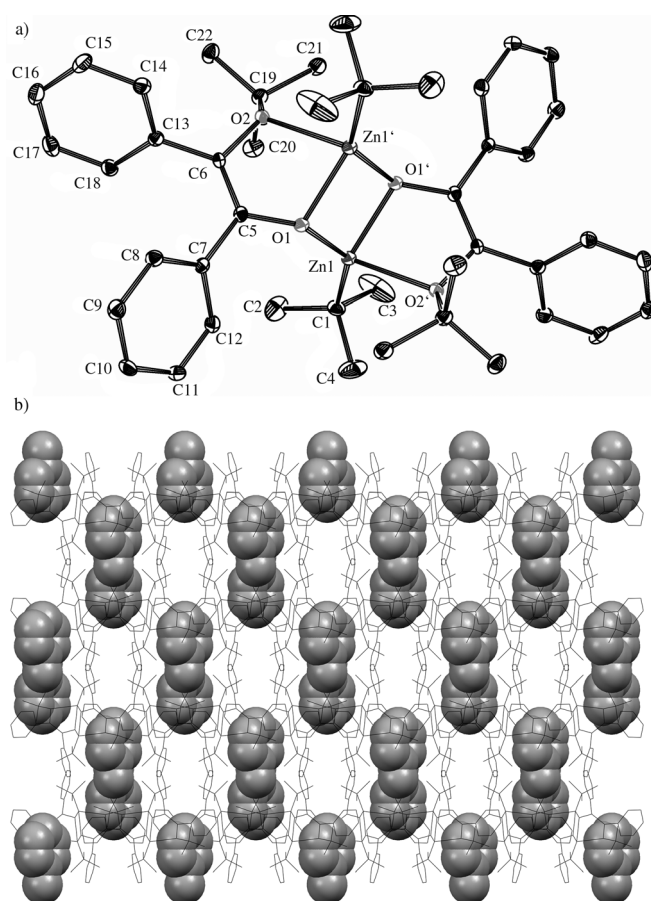


Figure 4. a) ORTEP diagram of the molecular structure of **1**<sub>2</sub> with thermal ellipsoids set at 35% probability; hydrogen atoms have been omitted for clarity. b) 1D channels of **1**<sub>2</sub> along the *c* axis with entrapped toluene molecules (shown in space-filling mode). Selected bond lengths [Å] for **1**<sub>2</sub>: Zn1–C1 1.991(2), Zn1–O1 1.999(1), Zn1–O1' 2.032 (2), Zn1–O2' 2.257(1), Zn1–O2 2.257(1).

idyl)ethane at ambient temperature afforded the crystalline Lewis acid–base adduct  $\{[2]_{2}[1,2\text{-bis}(4\text{-pyridyl})\text{ethane}]\}_n$  (**3**).

Compound **1**<sub>2</sub> is a centrosymmetric dimer with the Zn<sub>2</sub>( $\mu$ -O)<sub>2</sub> bridges formed by the enolate oxygen atoms and with each zinc having a distorted tetrahedral geometry (Figure 4a). The Zn–O bridging bonds fall into the narrow range of 1.999–2.032 Å and the Zn–O distance (2.257(1) Å) involving the chelating *Or*Bu group is significantly longer. The C=C bond with 1.347(3) Å is characteristic for a normal double bond observed for zinc enolate complexes.<sup>[8]</sup> Analysis of the crystal structure of **3** revealed that coordination-driven self-assembly of the dimeric alkoxide [EtZn{PhC(O)C(OEt)Ph}]<sub>2</sub> units with the bipyridine spacer of an *anti* conformation leads to a novel zigzag-like coordination polymer (Figure 5b).

In the **2**<sub>2</sub> unit the *O*-alkylated dibenzoyl acts as a mono-anionic ligand with a bridging enolate oxygen atom and a chelating ethoxide group; the average C–C and C–O distances within this ligand are very close to those found for **1**.

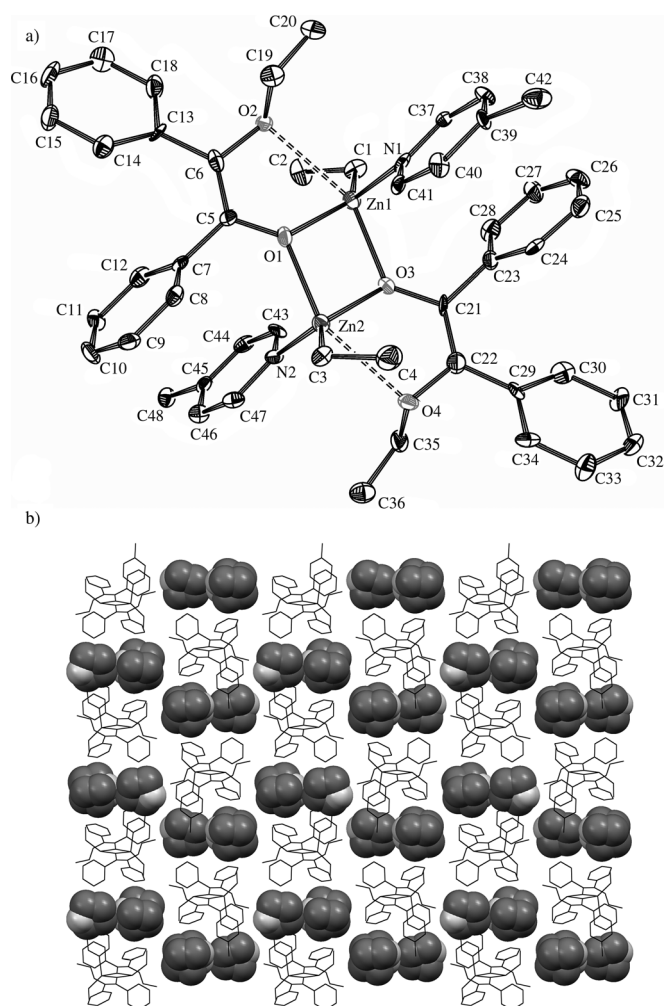


Figure 5. a) ORTEP diagram of the molecular structure of **3** with thermal ellipsoids set at 35% probability; hydrogen atoms have been omitted for clarity. b) 1D channels of **3** along the *c* axis with entrapped toluene molecules (shown in space-filling mode). Selected bonds lengths [Å] for **3**: Zn1–C1 1.976(8), Zn1–O1 2.025(5), Zn1–O2 2.669(6), Zn1–O3 2.125(5), Zn2–O1 2.120(6), Zn2–O3 2.020(6), Zn2–O4 2.674(6), Zn1–N1 2.101(7), Zn2–N2 2.065(7).

The pyridine ligands complete the coordination sphere of the EtZn centres with an average Zn–N bond length of 2.083 Å. The Zn–O distances within the central Zn<sub>2</sub>(μ-O)<sub>2</sub> ring in **3** differ slightly and range from 2.020–2.125 Å. The distances between the zinc centres and the ethoxide oxygen atoms are rather large with an average of 2.669 Å (drawn by dashed lines on Figure 5a) and they should be rather described as incipient bonding interactions.<sup>[19]</sup> Not surprisingly, this interaction essentially does not affect the coordination geometry of the zinc centres, which can be best described as severely distorted tetrahedrons. It should also be emphasised that compound **3** represents the first example of a coordination polymer with an alkylzinc–alkoxides aggregate as a node. Furthermore, analysis of the crystal structure of **1**<sub>2</sub> and **3** revealed that in both cases non-covalent interactions-driven self-assembly processes involving C–H–π and π–π in-

teractions between aromatic rings lead to 3D networks with slightly gated voids or open channels, respectively, filled by solvent molecules. The corresponding supramolecular arrangements are emphasised in the skeletal space filling diagrams presented in Figures 4b and 5b. Thus, the results additionally demonstrate that alkylzinc enolates derived from dibenzoyl can potentially act efficiently as predesigned secondary building blocks for the construction of coordination polymers and novel microporous architectures by coordination-driven and non-covalent interactions-driven self-assembly.

## Conclusion

In conclusion, we have performed for the first time systematic experimental and theoretical investigations of ZnR<sub>2</sub> (R = Me, Et and *t*Bu) with dibenzoyl as a non-innocent α-diketone ligand and revealed that the character of the metal-bonded R substituent as well as the reaction conditions, like temperature or the ratio of the reagents, significantly modulate the outcome of the reaction. The reaction involving ZnMe<sub>2</sub> did not lead to any alkylation products at ambient temperature, whereas the employment of Zn*t*Bu<sub>2</sub> resulted in full conversion of dbz to the *O*-alkylated product already at –20 °C. The addition of ZnEt<sub>2</sub> to dibenzoyl appeared particularly complex and monitoring of the dibenzoyl conversion over the entire course of the alkylation reaction revealed the product inhibition effect, which highlights possible participation of multiple equilibria of different zinc alkoxide aggregates. The reported results should be helpful for a rational organozinc reagent design and shall stimulate further experimental and theoretical investigations to clarify the correlation between structure and activity of organozinc species. In addition, the alkylzinc alkoxides derived from dibenzoyl appear intriguing metallotectons for the construction of coordination polymers and novel microporous architectures by coordination-driven and non-covalent interactions-driven self-assembly. Further studies on the reactivity of α-diketone/ZnR<sub>2</sub> systems and factors controlling the degree of aggregation of alkylzinc alkoxides are in progress.

## Experimental Section

**General methods:** All reactions were conducted under a nitrogen atmosphere by using standard Schlenk techniques. Diethylzinc (pure), dimethylzinc (2 M solution in toluene), 1,2-bis(4-pyridyl)ethane and dibenzoyl of commercial grade (Sigma–Aldrich), were used. Di-*tert*-butylzinc (1.4 M solution in toluene) was prepared according to the literature procedure.<sup>[20]</sup> Solvents were carefully dried and distilled prior to use. NMR spectra were acquired on a Varian Mercury 400 MHz spectrometer. Low temperature and diffusivity measurements were performed on a Varian Inova 500 MHz instrument.

**Caution:** Zinc reagents (Me<sub>2</sub>Zn, Et<sub>2</sub>Zn, *t*Bu<sub>2</sub>Zn) used in the reactions described below are pyrophoric compounds reacting violently with oxygen and water. Special care must be taken when operating with these compounds.

**Diffusivity measurement:** Application of diffusion-ordered spectroscopy (DOSY), which has happened to become a very routine NMR technique lately, provided us with a reliable evidence of approximate size of the species existing in solution. As already discussed in antecedent works<sup>[13]</sup> the molecular weight can be straightforwardly obtained by combining Stokes–Einstein equation [Eq. (1)] and the relationship between molecular weight  $M$  and molar radius [Eq. (2)]. It has also been shown that these quantities are much alike for small molecules, which is the case in our system. DOSY measurements were performed in dry and degassed [D<sub>8</sub>]toluene as we exploited the fact that the physical properties of the diluted solution, namely density and viscosity, deviate only slightly from the properties of the pure solvent.<sup>[13]</sup> Solutions were prepared so that the concentration of the resulting species emerging in the course of the reaction was approximately 0.01 M. A pulsed field gradient double-stimulated echo convection-compensated sequence with total of 15 diffusion encoding gradients (ranging from 3–45 G cm<sup>-1</sup>, sine shaped, equal steps in gradient squared) was used and the total width of the gradient pulse was optimised to achieve attenuation of about 90% of the initial intensity of the signals. Overall, the key acquisition parameters were as follows: total length of gradient encoding pulses gradient: 2 ms, diffusion delay: 50 ms, gradient recovery delay: 1 ms, relaxation delay: 2 s. Steady-state scans in number of 16 were performed prior to data acquisition. The sample was allowed to equilibrate in the set temperature (298 K), controlled by a VT module. Spinner was turned off. Raw data were processed with a powerful DOSY toolbox, which is extensively described in the literature.<sup>[21]</sup>

**Computational details:** The geometry of all molecules was optimised by density functional theory<sup>[22]</sup> by using the Gaussian 09<sup>[23]</sup> package. Geometry optimisations were carried out by using standard gradient methods (Bery algorithm) with the M06-2X functional<sup>[24]</sup> and the Dunning-like aug-cc-pVDZ<sup>[25]</sup> double-zeta basis set. Optimisations were performed without constraints apart from the *s-cis* conformation of dibenzoyl, where the O–C–C–O dihedral angle was frozen (0.0°) (as a consequence, this geometry does not correspond to a minimum at the potential energy surface). To validate locations of stationary points, all freely optimised geometries were subjected to frequency calculations (by using analytical methods) at the same level of theory and in the same basis set as optimisations were performed. As a result, zero-point energies for all species apart from the *s-cis* conformation of dibenzoyl, were obtained. For all freely optimised geometries nuclear hessian had only positive eigenvalues (corresponding to energy minima). To improve the accuracy of the energetic results, single point DFT energy recalculations were performed on previously optimised structures by using the same exchange–correlation functional but with extension of the basis set to triple zeta quality—aug-cc-pVTZ.<sup>[25]</sup> These re-calculations were performed by using automatic correction for BSSE (basis set superposition error) with a counterpoise (Boys–Bernardi) method.<sup>[26,27]</sup> During all optimisations the aug-cc-pVDZ basis set was used. Spherical harmonics basis set functions were used throughout and the linear dependence of the basis set functions was not observed. To provide reliable results of both geometry optimisations and energy calculations grid used for numerical integration of the DFT equations (both self-consistent field and gradient/hessian) was extended to 126 radial points and 770 angular points per atom (which roughly corresponds to extension by a factor of two compared to the default Gaussian 09 options). At the stage of geometry optimisations, no correction for BSSE was introduced. This approximation is fully justified by further single-point energy re-calculations corrected for BSSE—in all cases BSSE was small (usually less than 4 kJ mol<sup>-1</sup>), so its influence on the resulting geometries is clearly insignificant. Final energetic relations were obtained by using results from re-calculations at the aug-cc-pVTZ level (corrected for BSSE) and ZPE computed at aug-cc-pVDZ level. Solvent effects were not included at any stage of the calculations (for the results of the DFT calculations see the Supporting Information).

**[*t*BuZn(PhC(O)C(O*t*Bu)Ph)] (1):** *t*Bu<sub>2</sub>Zn (87.7 mg, 0.49 mmol) in THF (0.35 mL) was added to a solution of dibenzoyl (0.104 g, 0.49 mmol) in THF (5 mL) at –78°C. The reaction mixture was left to warm up to room temperature and stirred for 2 h. After 24 h of crystallisation from THF/hexane at –15°C colourless crystals suitable for X-ray analysis were obtained in 70% yield. <sup>1</sup>H NMR (400 MHz, CDCl<sub>3</sub>, 20°C): δ = 1.28

(m, 18H; C(CH<sub>3</sub>)<sub>3</sub>), 7.51 (m, 4H; CH<sub>Ar</sub>), 7.69 (m, 2H; CH<sub>Ar</sub>), 7.97 ppm (m, 4H; CH<sub>Ar</sub>).

**Low temperature reaction of dibenzoyl with Et<sub>2</sub>Zn (2):** Et<sub>2</sub>Zn (0.09 mL, 0.111 g, 0.90 mmol) was added to a yellowish solution of dibenzoyl (0.189 g, 0.90 mmol) in diethyl ether (6 mL) at –20°C. The reaction mixture was slowly warmed up to room temperature over 1 h and the reaction mixture was stirred for further 36 h at room temperature. The solvent was removed from the resulting intensively yellow reaction mixture under reduced pressure to give the crude product **2** as a white solid. <sup>1</sup>H NMR (500 MHz, [D<sub>8</sub>]toluene, –30°C): δ = 0.40 (2H; Zn<sub>(1)</sub>CH<sub>2</sub>), 0.60 (brs, 2H; Zn<sub>(2)</sub>CH<sub>2</sub>), 0.92 (brs, 3H; Zn<sub>(2)</sub>CH<sub>2</sub>CH<sub>3</sub>), 1.10 (3H; Zn<sub>(1)</sub>CH<sub>2</sub>CH<sub>3</sub>), 1.64 (3H; O<sub>(1)</sub>CH<sub>2</sub>CH<sub>3</sub>), 1.70 (brs, 3H; O<sub>(2)</sub>CH<sub>2</sub>CH<sub>3</sub>), 3.54 (brs, 2H; O<sub>(2)</sub>CH<sub>2</sub>CH<sub>3</sub>), 3.67 (2H; O<sub>(1)</sub>CH<sub>2</sub>CH<sub>3</sub>), 6.70–8.20 ppm (m, 10H; CH<sub>Ar</sub>); <sup>13</sup>C NMR (500 MHz, [D<sub>8</sub>]toluene, 20°C): δ = 0.01 (br), 6.22 (br), 6.90, 10.49 (br), 13.37 (br), 15.16, 65.84, 80.69, 133.6, 133.8, 134.3 (d), 137.4, 139.4, 139.7, 142.0, 146.6, 208.8, 209.8 ppm. Then NaHCO<sub>3</sub> was added to the crude product and the resulting mixture was stirred for 30 min. Toluene (5 mL) was added and after evaporation of the solvents under reduced pressure the organic residue was analysed by <sup>1</sup>H NMR spectroscopy (for the data description see the text below and Figure S1a in the Supporting Information).

**Room-temperature reaction of dibenzoyl with Et<sub>2</sub>Zn (2 and 2’):** Et<sub>2</sub>Zn (0.09 mL, 0.111 g, 0.90 mmol) was added to a yellowish solution of dibenzoyl (0.189 g, 0.90 mmol) in diethyl ether (6 mL) at room temperature and the reaction mixture was stirred for 36 h. The solvent was removed from the resulting intensively yellow reaction mixture under reduced pressure to give a mixture of crude product **2** and **2’** as a white solid. The <sup>1</sup>H NMR spectrum of the reaction mixture was complicated and not informative, the alkylation products were identified spectroscopically after hydrolysis: NaHCO<sub>3</sub> was added to the crude product and the resulting mixture was stirred for 30 min. Toluene (5 mL) was added and after evaporation of solvents under reduced pressure the organic residue was analysed by <sup>1</sup>H NMR spectroscopy (for the data description see the text below and Figure S1b in the Supporting Information). The resulting <sup>1</sup>H NMR spectra of the organic residue obtained from hydrolysis of reaction mixture confirm the anticipated *O*-alkylated and *C*-alkylated products: 2-hydroxy-1,2-diphenylbutan-1-one (**2**) and 2-ethoxy-1,2-diphenylethanone (**2’**). The latter compound exists in a keto–enol equilibrium in a ratio of 1:1.5. 2-hydroxy-1,2-diphenylbutan-1-one (**2**): <sup>1</sup>H NMR (400 MHz, [D<sub>6</sub>]benzene, 20°C): δ = 0.80 (t, *J* = 7.3 Hz, 3H; CH<sub>3</sub>), 2.24 (m, 2H; CH<sub>2</sub>), 4.34 (brs, 1H; OH), 6.50–7.30 ppm (m, 10H; CH<sub>Ar</sub>); 2-ethoxy-1,2-diphenylethanone (**2’**), keto form: <sup>1</sup>H NMR ([400 MHz, [D<sub>6</sub>]benzene, 20°C): δ = 1.05 (t, <sup>3</sup>*J*(H,H) = 6.6 Hz, 3H; CH<sub>3</sub>), 3.34 (m, 2H; CH<sub>2</sub>), 5.41 (s, 1H; CH) 6.50–7.30 ppm (m, 10H; CH<sub>Ar</sub>); enol form: <sup>1</sup>H NMR (400 MHz, [D<sub>6</sub>]benzene, 20°C): δ = 0.99 (t, <sup>3</sup>*J*(H,H) = 7.3 Hz, 3H; CH<sub>3</sub>), 4.10 (q, <sup>3</sup>*J*(H,H) = 7.3 Hz, 2H; CH<sub>2</sub>), 5.77 (brs, 1H; OH), 6.50–7.30 ppm (m, 10H; CH<sub>Ar</sub>).

**{[1,2-bis(4-pyridyl)ethane]}<sub>n</sub> (3):** Et<sub>2</sub>Zn (0.45 mL, 0.90 mmol, 2 M solution in THF) was added to a solution of dibenzoyl (0.189 g, 0.90 mmol) and 1,2-bis(4-pyridyl)ethane (0.083 g, 0.45 mmol) in THF (5 mL) at –78°C. The reaction mixture was warmed up to room temperature. During this time precipitation of light yellow crystals was observed. The reaction mixture was stirred at room temperature for 2 h. The solvents were removed under reduced pressure. The remaining solid was dissolved in THF (1.5 mL) and hexane (1 mL) was added. The solution was left for crystallisation at room temperature. Colourless crystals suitable for X-ray analysis were obtained after 24 h in 75% yield. <sup>1</sup>H NMR (400 MHz, CDCl<sub>3</sub>, 20°C): δ = 0.85 (4H; ZnCH<sub>2</sub>CH<sub>3</sub>), 1.26 (6H; ZnCH<sub>2</sub>CH<sub>3</sub>), 1.30 (6H; OCH<sub>2</sub>CH<sub>3</sub>), 2.97 (m, 4H; CH<sub>2</sub>CH<sub>2</sub>), 3.88 (4H; OCH<sub>2</sub>CH<sub>3</sub>), 7.10 (m, 8H; CH<sub>Ar</sub>), 7.11 (m, 4H; CH<sub>pyridyl</sub>), 7.13 (m, 4H; CH<sub>Ar</sub>), 7.45 (m, 8H; CH<sub>Ar</sub>), 8.46 ppm (m, 4H; CH<sub>pyridyl</sub>).

**X-ray structure determination:** The data were collected at 100(2) K on a Nonius Kappa CCD diffractometer<sup>[28]</sup> by using graphite monochromated MoK<sub>α</sub> radiation (λ = 0.71073 Å). The crystals were mounted in a nylon loop in a drop of silicon oil to prevent the possibility of decay of the crystals during data collection. The unit cell parameters were determined from ten frames, then refined on all data. The data were processed with DENZO and SCALEPACK (HKL2000 package).<sup>[29]</sup> The structure was

solved by direct methods by using the SHELXS97<sup>[30]</sup> program and was refined by full matrix least-squares on  $F^2$  by using the program SHELXL97.<sup>[31]</sup> All non-hydrogen atoms were refined with anisotropic displacement parameters. The hydrogen atoms were introduced at geometrically idealised coordinates with a fixed isotropic displacement parameter equal to 1.5 (methyl groups) times the value of the equivalent isotropic displacement parameter of the parent carbon. CCDC-789748 (**1**) and CCDC-787086 (**3**) contain the supplementary crystallographic data for this paper. These data can be obtained free of charge from The Cambridge Crystallographic Data Centre via [www.ccdc.cam.ac.uk/data\\_request/cif](http://www.ccdc.cam.ac.uk/data_request/cif). For selected bond lengths see Tables S1 and S2 in the Supporting Information.

**1**:  $C_{44}H_{59}O_4Zn_2 \cdot C_6H_5CH_3$ ;  $M = 871.80$ ; crystal dimensions  $0.52 \times 0.38 \times 0.28$  mm<sup>3</sup>, monoclinic; space group  $C2/c$  (no. 15);  $a = 11.8700(4)$ ,  $b = 17.6520(10)$ ,  $c = 22.2180(11)$  Å;  $\beta = 94.885(3)^\circ$ ;  $V = 4638.4(4)$  Å<sup>3</sup>;  $Z = 4$ ;  $F(000) = 1848$ ;  $\rho_{\text{calcd}} = 1.248$  gm<sup>3</sup>;  $\mu(\text{MoK}\alpha) = 1.08$  mm<sup>-1</sup>;  $\theta_{\text{max}} = 27.48^\circ$ ; 5102 unique reflections; refinement converged at  $R1 = 0.0734$ ;  $wR2 = 0.0928$  for all data and 263 parameters ( $R1 = 0.0395$ ,  $wR2 = 0.0846$  for 3502 reflections with  $I > 2\sigma(I)$ ); goodness-of-fit on  $F^2$  was equal 0.998; a weighting scheme  $w = [\sigma^2(F_o^2 + (0.0418P)^2 + 3.1964P)]^{-1}$  where  $P = (F_o^2 + 2F_c^2)/3$  was used in the final stage of refinement; residual electron density = +0.60/−0.50 e Å<sup>-3</sup>.

**3**:  $C_{48}H_{52}N_2O_4Zn_2 \cdot 3C_4H_8O$ ;  $M = 1068.01$ ; crystal dimensions  $0.42 \times 0.34 \times 0.24$  mm<sup>3</sup>, monoclinic; space group  $P21/c$  (no. 14);  $a = 10.5689(4)$ ,  $b = 19.6178(9)$ ,  $c = 26.3051(9)$  Å;  $\beta = 97.050(2)^\circ$ ;  $V = 5412.8(4)$  Å<sup>3</sup>;  $Z = 4$ ;  $F(000) = 2264$ ;  $\rho_{\text{calcd}} = 1.311$  gm<sup>3</sup>;  $\mu(\text{MoK}\alpha) = 0.94$  mm<sup>-1</sup>;  $\theta_{\text{max}} = 23.82^\circ$ ; 8287 unique reflections; refinement converged at  $R1 = 0.1488$ ;  $wR2 = 0.1822$  for all data and 654 parameters ( $R1 = 0.0689$ ,  $wR2 = 0.1526$  for 4370 reflections with  $I > 2\sigma(I)$ ); goodness-of-fit on  $F^2$  was equal 1.058; a weighting scheme  $w = [\sigma^2(F_o^2 + (0.0418P)^2 + 3.1964P)]^{-1}$  where  $P = (F_o^2 + 2F_c^2)/3$  was used in the final stage of refinement; residual electron density = +0.84/−0.66 e Å<sup>-3</sup>.

## Acknowledgements

This work was supported by the Ministry of Science and Higher Education (grant No. N N204 164336), the Interdisciplinary Centre for Mathematical and Computational Modelling (M.L.) and the European Union in the framework through the Warsaw University of Technology Development Programme of ESF (M.K.).

- [1] For example, see: a) A. Alberts, H. Wynberg, *J. Am. Chem. Soc.* **1989**, *111*, 7265–7266; b) K. Soai, T. Shibata, H. Morioka, K. Choji, *Nature* **1995**, *378*, 767–768; c) T. Rosner, P. J. Sears, W. A. Nugent, D. G. Blackmond, *Org. Lett.* **2000**, *2*, 2511–2513; d) T. Kawasaki, Y. Matsumura, T. Tsutsumi, K. Suzuki, M. Ito, K. Soai, *Science* **2009**, *324*, 492–495; e) B. M. Trost, A. Fettes, B. T. Shireman, *J. Am. Chem. Soc.* **2004**, *126*, 2660–2661; f) N. Chinkov, A. Warm, E. M. Carreira, *Angew. Chem.* **2011**, *123*, 3014–3018; *Angew. Chem. Int. Ed.* **2011**, *50*, 2957–2961.
- [2] For example, see: K. Soai, T. Shibata, I. Sato, *Acc. Chem. Res.* **2000**, *33*, 382–390; F. G. Buono, D. G. Blackmond, *J. Am. Chem. Soc.* **2003**, *125*, 8978–8979; I. D. Gridnev, J. M. Serafimov, J. M. Brown, *Angew. Chem.* **2004**, *116*, 4992–4995; *Angew. Chem. Int. Ed.* **2004**, *43*, 4884–4887; D. G. Blackmond, *Proc. Natl. Acad. Sci. USA* **2004**, *101*, 5732–5736; I. D. Gridnev, J. M. Brown, *Proc. Natl. Acad. Sci. USA* **2004**, *101*, 5727–5731; J. Klankermayer, I. D. Gridnev, J. M. Brown, *Chem. Commun.* **2007**, 3151–3153; L. Schiaffino, G. Ercolani, *Chem. Eur. J.* **2010**, *16*, 3147–3156; M. Quaranta, T. Gehring, B. Odell, J. M. Brown, D. G. Blackmond, *J. Am. Chem. Soc.* **2010**, *132*, 15104–15107.
- [3] M. Kitamura, S. Okada, S. Suga, R. Noyori, *J. Am. Chem. Soc.* **1989**, *111*, 4028–4036; L. Pu, H. Yu, *Chem. Rev.* **2001**, *101*, 757–824.
- [4] J. Lewiński, W. Marciniak, Z. Ochal, J. Lipkowski, I. Justyniak, *Eur. J. Inorg. Chem.* **2003**, 2753–2755.
- [5] See for example: a) G. van Koten, K. Vrieze, *Adv. Organomet. Chem.* **1982**, *21*, 151–239; b) W. Kaim, *Acc. Chem. Res.* **1985**, *18*, 160–166; c) R. J. Baker, C. Jones, *Coord. Chem. Rev.* **2005**, *249*, 1857–1869; d) N. J. Hill, I. Vargas-Baca, A. H. Cowley, *Dalton Trans.* **2009**, 240–253; e) P. J. Bailey, C. M. Dick, S. Farbe, S. Parsons, L. J. Yellowlees, *Dalton Trans.* **2006**, 1602–1610; f) I. L. Fedushkin, A. A. Skatova, S. Y. Ketkov, O. V. Eremenko, A. V. Piskunov, G. K. Fukin, *Angew. Chem.* **2007**, *119*, 4380–4383; *Angew. Chem. Int. Ed.* **2007**, *46*, 4302–4305; g) J. Lewiński, K. Suwała, M. Kubisiak, Z. Ochal, I. Justyniak, J. Lipkowski, *Angew. Chem.* **2008**, *120*, 8006–8009; *Angew. Chem. Int. Ed.* **2008**, *47*, 7888–7891.
- [6] a) T. Carofiglio, P. G. Cozzi, C. Floriani, A. Chiesi-Villa, *Organometallics* **1993**, *12*, 2726–2736; b) G. Quinkert, H. Becker, M. Del Grosso, G. Dambacher, *Tetrahedron Lett.* **1993**, *34*, 6885–6888.
- [7] a) G. H. Spikes, E. Bill, T. Weyhermüller, K. Wieghardt, *Angew. Chem.* **2008**, *120*, 3015–3019; *Angew. Chem. Int. Ed.* **2008**, *47*, 2973–2977; b) G. H. Spikes, S. Sproules, E. Bill, T. Weyhermüller, K. Wieghardt, *Inorg. Chem.* **2008**, *47*, 10935–10944.
- [8] For the synthesis and structure characterisation of zinc enolates see, for example: a) M. R. P. van Vliet, G. van Koten, P. Buysingh, B. H. T. Jastrzebski, A. L. Spek, *Organometallics* **1987**, *6*, 537–546; b) S. C. Goel, M. Y. Chiang, W. E. Buhro, *Inorg. Chem.* **1990**, *29*, 4646–4652; c) C. Bolm, J. Müller, M. Zehnder, M. A. Neuburger, *Chem. Eur. J.* **1995**, *1*, 312–317; M. L. Hlavinka, J. R. Hagadorn, *Organometallics* **2006**, *25*, 3501–3507; d) M. L. Hlavinka, J. R. Hagadorn, *Organometallics* **2005**, *24*, 4116–4118; J. F. Greco, M. J. McNevin, R. K. Shoemaker, J. R. Hagadorn, *Organometallics* **2008**, *27*, 1948–1953.
- [9] a) E. Erdik, *Organozinc Reagents in Organic Synthesis*, CRC Press, Boca Raton, **1996**; b) P. Knochel, R. D. Singer, *Chem. Rev.* **1993**, *93*, 2117–2188; c) H. Y. Kim, L. Salvi, P. J. Carroll, P. J. Walsh, *J. Am. Chem. Soc.* **2010**, *132*, 402–412.
- [10] L. E. Garner, H. Zhu, M. L. Hlavinka, J. R. Hagadorn, E. Y.-X. Chen, *J. Am. Chem. Soc.* **2006**, *128*, 14822–14823.
- [11] The presence of a small amount of the alkylated product may be attributed to local fluctuations of concentrations of reagents during the addition.
- [12] Q. Shen, K. Hagen, *J. Phys. Chem.* **1987**, *91*, 1357–1360; Z. Pawelka, A. Koll, T. Zeegers-Huyskens, *J. Mol. Struct.* **2001**, *597*, 57–66.
- [13] D. Li, G. Kagan, R. Hopson, P. G. Williard, *J. Am. Chem. Soc.* **2009**, *131*, 5627–5634; A. Macchioni, G. Ciancaleoni, C. Zuccaccia, D. Zuccaccia, *Chem. Soc. Rev.* **2008**, *37*, 479–489.
- [14] P. G. Cozzi, J. Rudolph, C. Bolm, P.-O. Norrby, C. Tomasini, *J. Org. Chem.* **2005**, *70*, 5733–5736.
- [15] J. M. Klerks, J. T. B. H. Jastrzebski, G. van Koten, K. Vrieze, *J. Organomet. Chem.* **1982**, *224*, 107–119; E. Wissing, E. Rijnberg, P. A. van der Schaaf, K. van Gorp, J. Boersma, G. van Koten, *Organometallics* **1994**, *13*, 2609–2615; I. J. Blackmore, V. C. Gibson, P. B. Hitchcock, C. W. Rees, D. J. Williams, A. J. P. White, *J. Am. Chem. Soc.* **2005**, *127*, 6012–6020.
- [16] J. Lewiński, W. Marciniak, J. Lipkowski, I. Justyniak, *J. Am. Chem. Soc.* **2003**, *125*, 12698–12699; J. Lewiński, W. Bury, M. Dutkiewicz, M. Maurin, I. Justyniak, J. Lipkowski, *Angew. Chem.* **2008**, *120*, 583–586; *Angew. Chem. Int. Ed.* **2008**, *47*, 573–576.
- [17] J. Lewiński, Z. Ochal, E. Bojarski, E. Tratkiewicz, I. Justyniak, J. Lipkowski, *Angew. Chem.* **2003**, *115*, 4791–4794; *Angew. Chem. Int. Ed.* **2003**, *42*, 4643–4646; J. Lewiński, K. Suwała, T. Kaczorowski, M. Gałęzowski, D. T. Gryko, I. Justyniak, J. Lipkowski, *Chem. Commun.* **2009**, 215–217.
- [18] J. Lewiński, W. Bury, I. Justyniak, J. Lipkowski, *Angew. Chem.* **2006**, *118*, 2938–2941; *Angew. Chem. Int. Ed.* **2006**, *45*, 2872–2875; J. Lewiński, M. Dranka, W. Bury, W. Śliwiński, I. Justyniak, J. Lipkowski, *J. Am. Chem. Soc.* **2007**, *129*, 3096–3098.
- [19] For an extended discussion on trajectory for the approaching ligand on the metal fifth coordinate site, see: J. Lewiński, J. Zachara, I. Justyniak, *Chem. Commun.* **2002**, 1586–1587.
- [20] H. Lehmkuhl, O. Olbrysch, *Justus Liebigs Ann. Chem.* **1975**, 1162–1175.
- [21] M. Nilsson, *J. Magn. Reson.* **2009**, *200*, 296–302.

- [22] W. Kohn, A. D. Becke, R. G. Parr, *J. Phys. Chem.* **1996**, *100*, 12974–12980.
- [23] Gaussian 09, Revision B.01, M. J. Frisch, G. W. Trucks, H. B. Schlegel, G. E. Scuseria, M. A. Robb, J. R. Cheeseman, G. Scalmani, V. Barone, B. Mennucci, G. A. Petersson, H. Nakatsuji, M. Caricato, X. Li, H. P. Hratchian, A. F. Izmaylov, J. Bloino, G. Zheng, J. L. Sonnenberg, M. Hada, M. Ehara, K. Toyota, R. Fukuda, J. Hasegawa, M. Ishida, T. Nakajima, Y. Honda, O. Kitao, H. Nakai, T. Vreven, J. A. Montgomery, Jr., J. E. Peralta, F. Ogliaro, M. Bearpark, J. J. Heyd, E. Brothers, K. N. Kudin, V. N. Staroverov, R. Kobayashi, J. Normand, K. Raghavachari, A. Rendell, J. C. Burant, S. S. Iyengar, J. Tomasi, M. Cossi, N. Rega, J. M. Millam, M. Klene, J. E. Knox, J. B. Cross, V. Bakken, C. Adamo, J. Jaramillo, R. Gomperts, R. E. Stratmann, O. Yazyev, A. J. Austin, R. Cammi, C. Pomelli, J. W. Ochterski, R. L. Martin, K. Morokuma, V. G. Zakrzewski, G. A. Voth, P. Salvador, J. J. Dannenberg, S. Dapprich, A. D. Daniels, Ö. Farkas, J. B. Foresman, J. V. Ortiz, J. Cioslowski, D. J. Fox, Gaussian, Inc., Wallingford CT, **2009**.
- [24] Y. Zhao, D. G. Truhlar, *Theor. Chem. Acc.* **2008**, *120*, 215–241.
- [25] N. B. Balabanov, K. A. Peterson, *J. Chem. Phys.* **2005**, *123*, 064107–064122.
- [26] S. F. Boys, F. Bernardi, *Mol. Phys.* **1970**, *19*, 553–566.
- [27] S. Simon, M. Duran, J. J. Dannenberg, *J. Chem. Phys.* **1996**, *105*, 11024–11031.
- [28] KappaCCD Software, Nonius B. V., Delft (The Netherlands), **1998**.
- [29] Z. Otwinowski, W. Minor, *Methods Enzymol.* **1997**, *276*, 307–326.
- [30] SHELXS97: G. M. Sheldrick, *Acta Crystallogr. Sect. A* **1990**, *46*, 467–473.
- [31] SHELXL97: G. M. Sheldrick, University of Göttingen, Göttingen (Germany), **1997**.

Received: June 28, 2011  
Published online: September 28, 2011